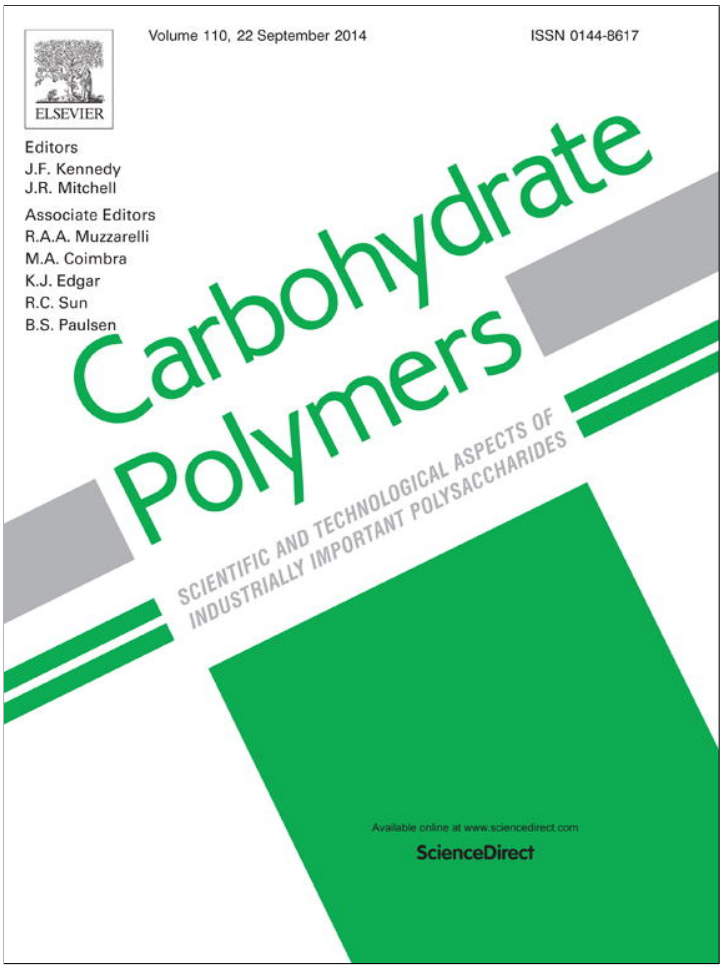

Carbohydrate Polymers 110 (2014) 78–86

Contents lists available at ScienceDirect

Carbohydrate Polymers

journal homepage: www.elsevier.com/locate/carbpol

Synthesis and electrical properties of polyaniline/iota-carrageenan biocomposites

Alejandro Vega-Rios, Jorge L. Olmedo-Martínez, Bárbara Farías-Mancilla, Claudia A. Hernández-Escobar, E. Armando Zaragoza-Contreras*

Centro de investigación en Materiales Avanzados, S.C. Miguel de Cervantes No. 120, Complejo Industrial Chihuahua, Chihuahua, Chih., Mexico

ARTICLE INFO

Article history:
Received 24 June 2013
Received in revised form 4 March 2014
Accepted 20 March 2014
Available online 3 April 2014

Keywords:
Biocomposite
Carrageenan
Electro-activity
Polyaniline

ABSTRACT

Polyaniline/iota-carrageenan (ι-CGN) biocomposites were synthesized *via in situ* methodology using ammonium persulfate as the oxidizing agent. Both ionic (band at 1131 cm^{-1}) and hydrogen bond (bands at 2500 and 3500 cm^{-1}) interactions between polyaniline and ι-CGN were determined by infrared spectroscopy. Such intermolecular interactions provided the biocomposites with a cross-linked structure that provided the materials with hydrogel behavior. Biocomposite electro-conductivity, determined by the 4-probe technique, was in the range of semiconductors (10^{-3} to 10^{-2} S cm^{-1}); whereas electro-activity, assessed by cyclic voltammetry, showed the oxidation–reduction transitions typical of polyaniline. Based on the properties of polyaniline and ι-CGN, some applications for the new materials in the field of biosensor design, electrochemical capacitors, or tissue engineering scaffolds are possible. It is worth saying that both electro-conductive and electro-active properties of polyaniline/ι-CGN biocomposites are reported here for the first time.

1. Introduction

Conducting polyaniline (PAni) has long been mixed with thermoplastic polymers to overcome processability limitations derived from its infusibility and poor solubility in common solvents. Polyaniline/thermoplastic composites are quite popular because depending on the thermoplastic matrix, conducting composites with different attributes can be obtained (Cai & Chen, 1998; Haberko et al., 2005; Pereira da Silva, Córdoba de Torresi, & Torresi, 2007; Pud, Ogurtsov, Korzhenko, & Shapoval, 2003; Sun, Shi, Chu, Xu, & Liu, 2012). However, because of the limited availability of fossil resources, renewable bioresources, such as polysaccharides, are ideal alternative raw materials because of their natural abundance (Rinaudo, 2008) and biodegradability (Šimkovic, 2013). Taking this into consideration, cellulose derivatives, for instance, have been used to produce PAni biocomposites with a wide variety of possible applications (Lee, Chung, Kwon, Kim, & Tze, 2012; Hu, Chen, Yang, Liu, & Wang, 2011; Liu, Zhou, Qian, Shen, & An, 2013; Müller et al., 2012; Qaiser, Hyland, & Patterson, 2011).

Carrageenan (CGN) is the generic name for a family of carbohydrate extracts composed of sulfated galactose units. It is a product derived from red algae *Chondrus crispus* (*Filo Rhodophita*) (Di Rosa, 1972), although other sources are also available (Al-Alawi, Al-Marhubi, Al-Belushi, & Soussi, 2011; Freile-Pelegrín & Robledo, 2008; Hilliou, Larontonda, Sereno, & Gonçalves, 2006; Tuvikene et al., 2009). Carrageenan is a high molecular weight linear polysaccharide comprising repeating galactose units and 3,6-anhydrogalactose, both sulfated and non-sulfated, joined by alternating α-(1,3) and β-(1,4) glycosidic links. The most common types of carrageenan are traditionally identified by a Greek prefix called ι(iota)-, κ(kappa)-, or λ(lambda)-carrageenan, which have been very well differentiated (Volery, Besson, & Schaffer-Lequart, 2004). Carrageenans are often used as thickening agents, stabilizers, and emulsifiers in foods and gel-like products; however, in recent years more advanced technological applications for CGN have been explored (Coggins et al., 2000; Fujishima, Matsuo, Takatori, & Uchida, 2008; Gaweł et al., 2013; Pourjavadi, Harzandi, & Hosseinzadeh, 2004; Prasad & Kadokawa, 2010).

Polyaniline/carrageenan (PAni/CGN) systems have, in fact, been scarcely studied; to the best of our knowledge, the recent published work of Leppänen et al. is the only one published up to now concerning this topic (Leppänen, Xu, Liu, Wang, Pesonen, & Willför, 2013). In that communication, this group reported the synthesis *via* enzymatic pathway of PAni in combination with κ-carrageenan (κ-CGN), and other polysaccharides, to produce conducting biocomposites. Herein, we report for the first time thermal,

* Corresponding author. Tel.: +52 614 439 4811; fax: +52 614 439 1130.
E-mail address: armando.zaragoza@cimav.edu.mx (E.A. Zaragoza-Contreras).

http://dx.doi.org/10.1016/j.carbpol.2014.03.068
0144-8617/

electro-conductive, and electro-active properties of PAni/ι-CGN biocomposites. This work was inspired by the use of sulfate or sulfonate anions as doping groups of PAni (Chao et al., 2008; Paul & Pillai, 2000; Roy et al., 2002; Tsutsumi, Yamashita, & Oishi, 1997) and by the possibility to produce functional composites from biorenewable resources as an alternative to classical thermoplastic composites. The significance of using ι-CGN in this study lies in the following aspects: (a) the high content of sulfate groups by repeating unit (two in average) and (b) the disposition of the sulfate groups along the molecule which facilitate the interaction with other charged species, in the present case, with the anilinium cations of polyaniline. Based on the literature, the resulting materials potentially present properties such as biodegradability, biocompatibility, and processability because of the carrageenan host matrix (Lim et al., 2010; Sharma, Bhat, Vishnoi, Nayak, & Kumar, 2013; Van, 2002) and electro-conductive and electro-active properties because of the inclusion of PAni (Bagheri, Didehban, Razmi, & Entezami, 2004; Mirmohseni, Salari, & Nabavi, 2006; Vega-Rios, Hernández-Escobar, Zaragoza-Contreras, & Kobayashi, 2013). This set of properties allows us to visualize potential applications for the composites; for example, in biosensor design, electrochemical capacitors, drug delivery, development of membranes for removing heavy ions, conductive hydrogel, or tissue engineering scaffolds.

2. Material and methods

2.1. Materials

Aniline (Acros Organics, 99.8%) was distilled under reduced pressure before use. ι-CGN (Aldrich Co., Type II, C-1138 commercial grade), hydrochloric acid (J.T. Baker, 36.5%), water (Golden Bell, specific conductance at 25 °C 2 μΩ/cm), ammonium persulfate (Aldrich Co., ≥98%), sodium hydroxide (Aldrich Co., ≥99%), and ethanol (J.T. Baker, 96%) were used as received.

2.2. Biocomposite synthesis

In a typical experiment, ι-CGN (5×10^{-3} g mL^{-1}) was dissolved in warm water (40 °C) and then thoroughly mixed with a solution of aniline-hydrochloric acid (anilinium chloride salt). The solution was left to air dry under ambient conditions and the oxidizing agent, ammonium persulfate (APS), equivalent to a molar ratio 1.0:1.25 (aniline:APS) was added and perfectly mixed. The system was placed under refrigeration (−2 °C) and left to polymerize for 48 h. The colorless system turned immediately into a gel, which gradually acquired a green color, evidencing the production of PAni emeraldine salt (conducting form of PAni). A scheme of the ionic interaction aniline/ι-CGN is illustrated in Fig. 1. The recipes for the synthesis of the biocomposites and blank of PAni are summarized in Table 1.

PAni conversion was determined gravimetrically as follows: first, the product (PAni/ι-CGN biocomposite) was left to air dry under ambient conditions. Then 0.5 g of solids were finely ground and dispersed in 100 mL of distilled water. The dispersion was sonicated for 10 min to hydrate the material. Then, 3.0 mL of sodium hydroxide solution (0.1 M) was added to obtain dedoped PAni (emeraldine base of dark-blue color). The mixture was stirred and warmed at 70 °C for 15 h. Subsequently, the solids were recovered by filtration (filter paper) and washed with warm water to remove residues of ι-CGN. Finally, the PAni recovered was re-doped by adding hydrochloric acid (10 mL, 0.1 M) and dried at 60 °C under

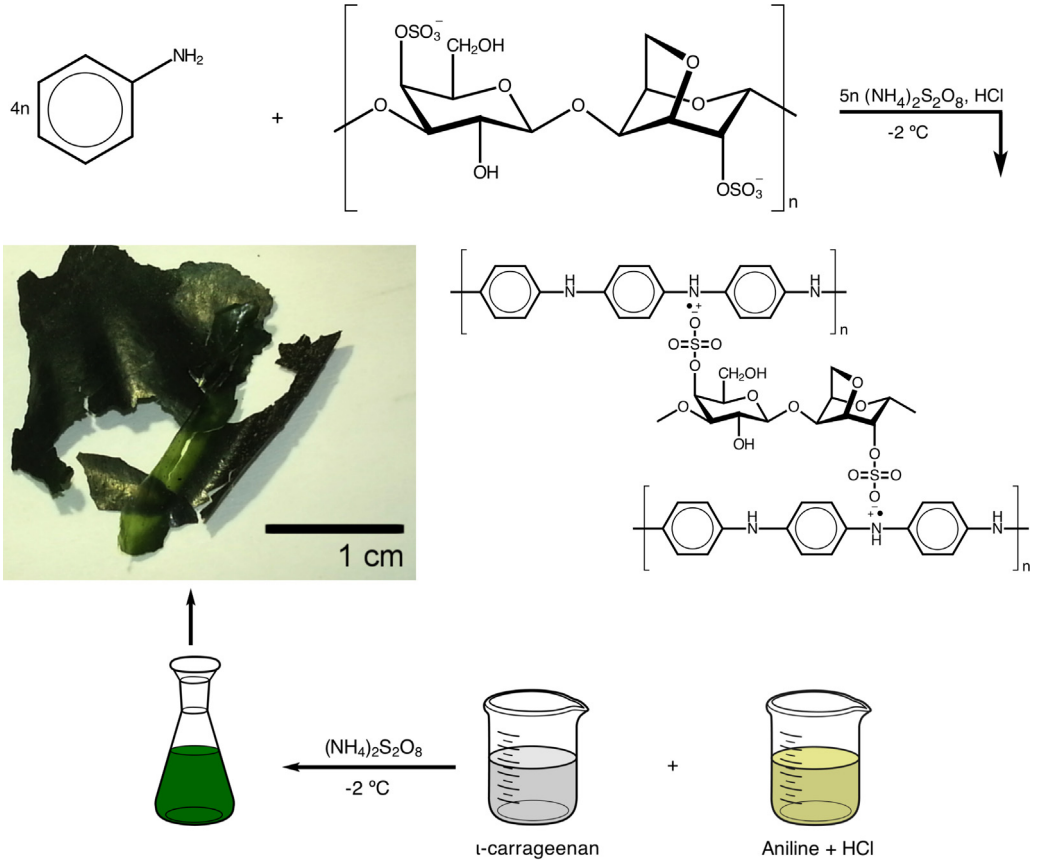

Fig. 1. Route of synthesis of PAni/ι-CGN biocomposites. Ammonium persulfate was used as the oxidizing agent. The method was designed to favor ionic interaction between anilinium (PAni) and sulfate (ι-CGN) ions.

Table 1
Synthesis of the PAni/ι-CGN biocomposites and blank of PAni.

Sample	ι-Carrageenan ($g\,mL^{-1}$)	Aniline (M)	HCl (M)	APS (M)	PAni[a] (wt%)
PAni	–	1	1	1.250	–
C1	5×10^{-3}	0.05	0.05	0.0625	21.2
C2	5×10^{-3}	0.10	0.10	0.125	28.7
C3	5×10^{-3}	0.15	0.15	0.1875	37.0
C4	5×10^{-3}	0.20	0.20	0.250	50.5
C5	5×10^{-3}	0.25	0.25	0.3125	62.6
C6	5×10^{-3}	0.50	0.50	0.625	81.3

[a] PAni content in the biocomposites calculated using Eq. (1).

reduced pressure for 24 h. The content of PAni in the biocomposites (wt%) was calculated as shown in Eq. (1):

$$\text{PAni}\,(\text{wt\%}) = \frac{W_f - W_1}{W_0} \quad (1)$$

where W_0 is the weight of PAni/ι-CGN biocomposites, W_1 is the weight of filter and W_f is the weight of dry PAni with filter.

2.3. Characterization

Scanning electron microscopy in transmission mode (STEM) was performed in a field emission electron microscope (JSM-7401F; JEOL) at 30 kV. To prepare the samples of biocomposite, 0.01 g of dried and finely ground biocomposite was dispersed in 100 mL of water; then, the dispersion was sonicated for 10 min to hydrate and disperse the material. A drop of hydrogel dispersion was placed on a holey-carbon-copper grid and left to air dry under ambient conditions. In the case of the pure PAni (see supplementary information), two drops of dispersion of the original polymerization were dispersed and sonicated for 5 min in 30 mL of water. Subsequently, a drop of the new dispersion was placed on a holey-carbon-copper grid and left to dry.

Fourier infrared spectroscopy (FTIR) spectra were recorded with a Fourier transform spectrometer (Spectrum GX, Perkin Elmer) using attenuated total reflection (ATR) technique at room temperature. Thermal degradation of the biocomposites, PAni and ι-CGN was characterized using a thermogravimetric analyzer (TGA Q500, TA Instruments). Measurements were achieved using 10 mg of sample, heating from laboratory temperature to 800 °C, at a heating rate of 10 °C min^{-1} in argon atmosphere. Electrical conductivity was determined by the 4-point technique using a conductivity

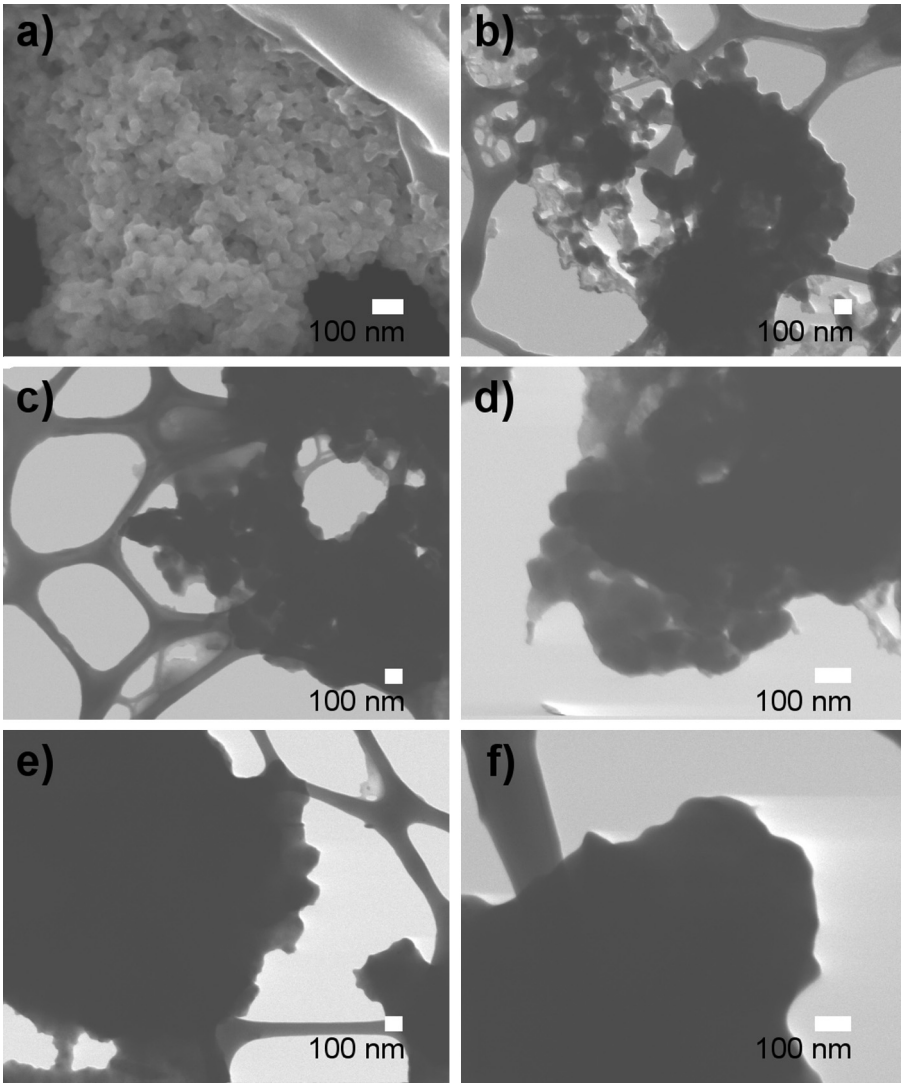

Fig. 2. Images of scanning electron microscopy in transmission mode (STEM) of (a) pure PAni, obtained from the oxidative polymerization of anilinium chloride salt, and (b)–(f) biocomposites synthesized with different aniline molar loading: (b) 0.05, (c) 0.1, (d) 0.15, (e) 0.2, and (f) 0.25.

meter (34410A 6 1/2 Digit, Agilent). Pellets of each biocomposite and pure PAni (1.5 mm width and 12 mm diameter) were prepared by compression (6900 kPa). The biocomposites were additionally characterized by cyclic voltammetry (CV) using a potentiostate analyzer (model 1260 plus 1287, Solartron). Electrochemical measurements were performed in a standard three-electrode cell at room temperature, using Pt square foil (area = 0.75 cm^2) as the counter electrode, and Ag/AgCl/saturated KCl as the reference electrode. The electrolyte was a sulfuric acid (H_2SO_4) solution 0.1 M. All analyses were performed at a scan rate of 50 mV s^{-1} by sweeping the potential between −500 and +1000 mV against Ag/AgCl reference electrode. Working electrodes were made with carbon paste depositing 5 mg of the biocomposite.

3. Results and discussion

3.1. Morphology

In the biocomposite synthesis, anilinium chloride and ι-CGN were mixed so that the anilinium cations and the sulfonate anions of ι-CGN formed sulfonate anilinium by ion interchange. An equivalent process was performed in the report of Leppänen et al. (2013) for PAni/κ-CGN composite and for sulfonated polymers like polystyrenesulfonate (Luo, Jiang, Wu, Chen, & Liu, 2012; Roy et al., 2002; Sun et al., 2012; Wang, Liu, Feng, Guo, & Sun, 2008) or lignosulfonate (Lü, Wang, & Cheng, 2010).

Microscopy images of the pure PAni and the biocomposites C1 to C5 are portrayed in Fig. 2 (micrograph for C6 is included in the Supplementary Material Section, Fig. S1). As observed, the pure PAni obtained from the oxidative polymerization of anilinium chloride, using APS as the oxidizing agent, is formed from semi-spherical agglomerated particles of the order of 30 nm. In the case of the biocomposites, a tendency to form coarse lumps was evident, and although the semi-spherical particles observed were larger, in the order of *ca.* 100 nm, this still indicated that the PAni in the biocomposites preserved the tendency to form particles as in the pure form. Concerning the macro-scale, the biocomposites formed, depending on the PAni content, semi-transparent-brittle films as seen in Fig. 1. These materials swell slightly in water at ambient conditions, but under progressive heating (ambient to 80 °C) the hydrogels absorbed more water without reaching solubilization (swelling was not studied). Under these conditions ι-CGN is water-soluble. Subsequent addition of sodium hydroxide (at room temperature) followed by warming to 40 °C, produced ι-CGN solubilization. That is, the sodium cations exchanged with the anilinium cations eliminating the ionic interaction between PAni and ι-CGN allowing the second to solve in the water and turning the PAni to the emeraldine base form (dark-blue) as mentioned above. These results support the notion that the PAni and the ι-CGN are forming a truly ionic cross-linked network with the constituents linked by ionic bonds between the anilinium cations and the sulfate anions and not merely by a simple physical mixture. It is worth saying that biocomposite brittleness may be reduced with the use of some plasticizer, a glycol, for example, to improve film handling for practical matters. This study is being conducted at the moment and will be reported shortly.

3.2. Infrared spectroscopy

The FTIR spectra of the biocomposites, ι-CGN and PAni are shown in Fig. 3. The main characteristic bands of ι-CGN are located at 3392 cm^{-1} (O—H bonds stretching vibrations forming intermolecular hydrogen bonds), 1638 cm^{-1} (O—H bond of water of crystallization), 1152 and 1024 cm^{-1} (C—O—H and C—O—C stretching vibrations), 1373 and 1214 cm^{-1} (asymmetric and symmetric vibration of $S{=}O_2$ group), 930 cm^{-1} (C—O of 3,6-anhydro-o-galactose) (Chopin & Whalen, 1993; Socrates, 2001; Turquois, Acquistapace, Vera, & Welti, 1997). ι-CGN is a carrageenan with two sulfate groups, one showing a band at 845 cm^{-1}, arising from the galactose-4-sulfate group, and the other one at 805 cm^{-1}, attributed to the anhydrogalactose-2-sulfate group. The spectra of κ-CGN (one sulfate group), ι-CGN, and λ-CGN (three sulfate groups) have been reported in literature (Gómez-Ordóñez & Rupérez, 2011; Pereira & Mesquita, 2003; Pereira, Sousa, Coelho, Amado, & Ribeiro-Claro, 2003; Turquois et al., 1997).

Infrared spectroscopy characterization of PAni has been widely discussed in the literature (Šeděnková, Trchová, Blinova, & Stejskal, 2006; Šeděnková, Trchová, & Stejskal, 2008; Trchová,

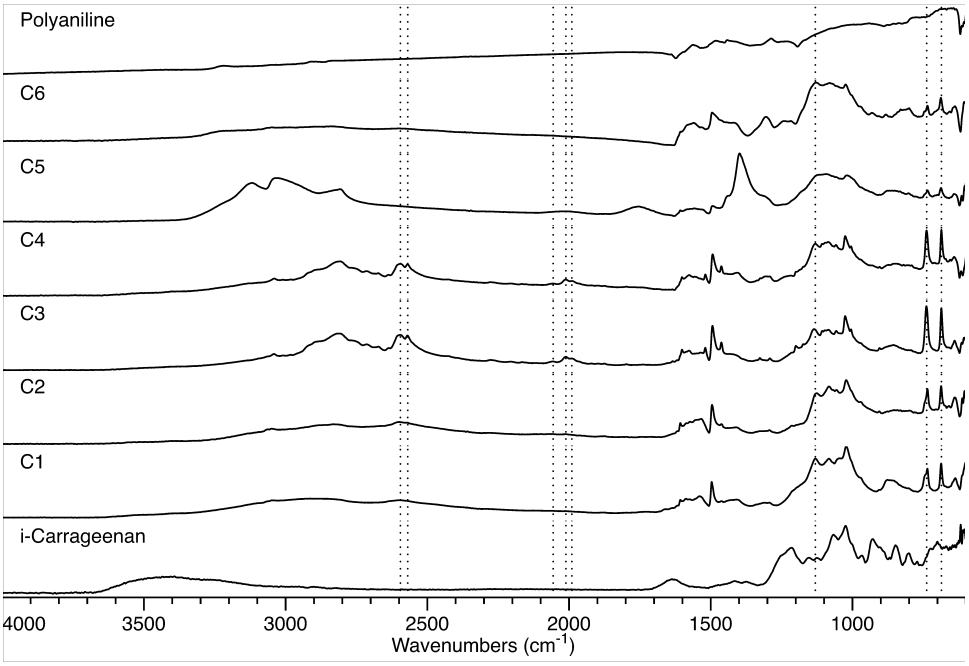

Fig. 3. Infrared spectroscopy spectra of ι-CGN, pure PAni and the PAni/ι-CGN biocomposites (C1 – 0.05 M, C2 – 0.1 M, C3 – 0.15 M, C4 – 0.2 M, C5 – 0.25 M, and C6 – 0.5 M).

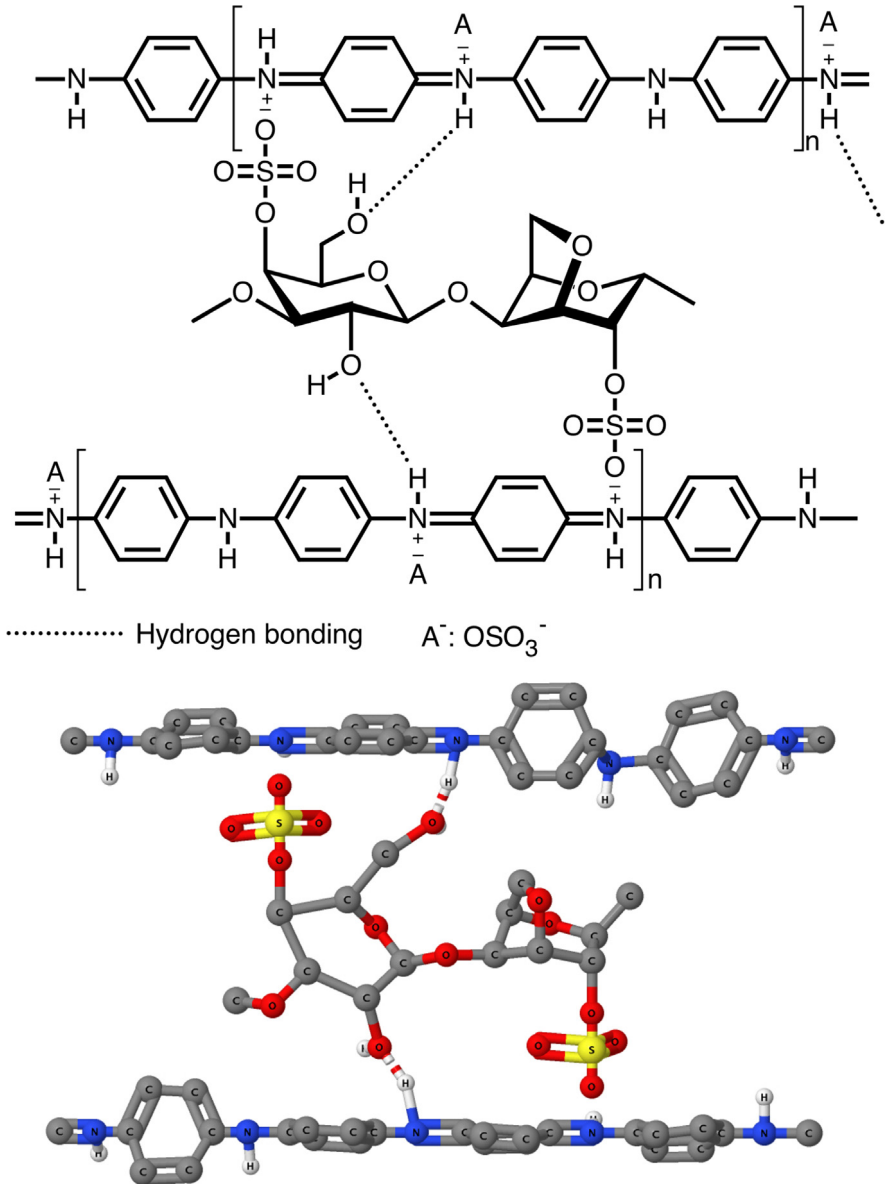

Fig. 4. Model of interaction ι-CGN–PAni, indicating both ionic interaction HN^+—OSO_3 and hydrogen bond interaction O—H—N^+.

Šeděnková, Tobolková, & Stejskal, 2004). The characteristic peaks of PAni appear at 1493 and 1575 cm^{-1}, these bands are ascribed to the stretching vibration of benzenoid and quinoid rings ($[(—B—NH—B—NH—)_y(—B—N═Q═N—)_{1-y}]_x$, where B and Q denote, respectively, C_6H_4 rings in the benzenoid and quinoid forms) (Ebrahim, Kashyout, & Soliman, 2007; Shi et al., 2012). The bands at 1260, 1307, and 1369 cm^{-1} are related to the stretching vibrations of charged nitrogen segments, and provide information about the charge delocalization in the PAni chains. Other major peaks are the deformations from the ring B and Q at 857 and 829 cm^{-1}, respectively (Trchová & Stejskal, 2011).

Concerning the biocomposites, the spectra showed the characteristic bands of both ι-CGN and PAni as discussed before. However, some important changes can be pointed out; for instance, the band at 3392 cm^{-1}, characteristic of O—H bonds present in ι-CGN, decreased in intensity and new peaks, in the region between 2500 and 3500 cm^{-1}, appeared. These changes suggested the occurrence of hydrogen bond interactions between OH groups of ι-CGN with NH groups of PAni. A similar behavior was observed by Yavuz, Uygun, and Kaplan Can (2011) in polyaniline and substituted polyanilines/chitosan composites. They reported the broadening of bands between 2878 and 3435 cm^{-1} caused by the hydrogen–oxygen interaction/binding between NH and OH groups of PAnis and chitosan, respectively. The new peaks, product of such interaction are observed at 2595 and 2569 cm^{-1}, ascribed to stretching vibrations of the imine hydrohalide group, reported by Socrates (2001) in the region between 2700 and 2330 cm^{-1}. Additionally, Socrates reported that imine hydrohalides present one or more bands of medium intensity in the region 2200–1800 cm^{-1}, which may be used to distinguish from amine hydrohalides. Particularly in this region, all PAni/ι-CGN biocomposites presented three peaks at 1990, 2011, and 2056 cm^{-1}, confirming that the imine hydrohalide group, which is present in the quinoid structure (Q), form hydrogen bonds between hydrogen of the imine hydrohalide and oxygen free pairs of electrons (see Supplementary Material Section, Fig. S2).

Two additional bands, at 686 and 738 cm^{-1}, are also observed in all biocomposites. These bands correspond, respectively, to the C—H vibration out-of-plane bending and to the vibration out-of-plane deformation of the monosubstituted phenylene ring. Bands

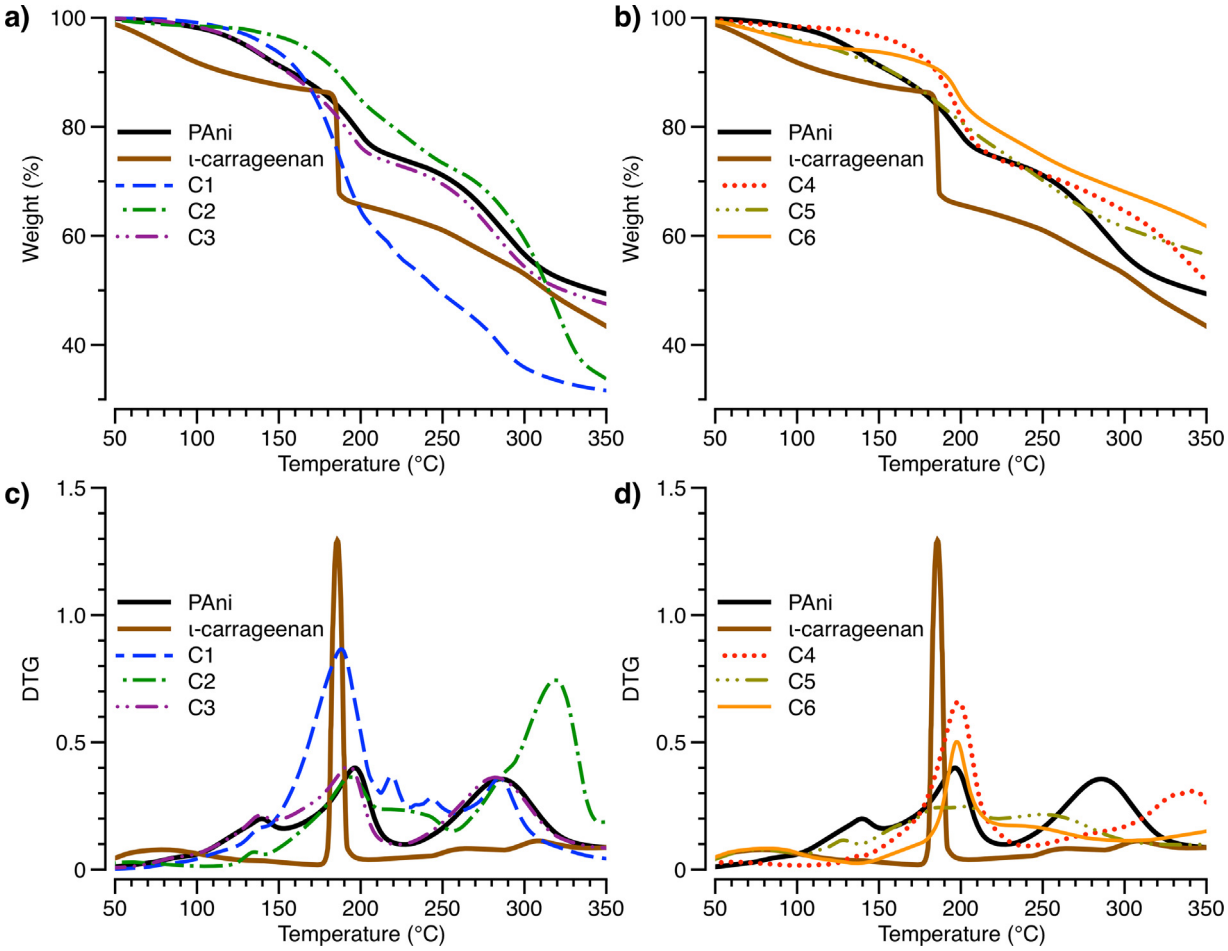

Fig. 5. Thermogravimetric profiles of ι-CGN, pure PAni and the PAni/ι-CGN biocomposites (C1 – 0.05 M, C2 – 0.1 M, C3 – 0.15 M, C4 – 0.2 M, C5 – 0.25 M, and C6 – 0.5 M).

in these regions were reported for PAni, when it was polymerized in the presence of a weak acid, such as acetic acid (Trchová & Stejskal, 2011). These two peaks suggested the occurrence of a complementary interaction, different from the polymerization of PAni when the aniline is protonated with a strong acid. In the present case, these two bands support the previous discussion concerning the formation of hydrogen bonds between the oxygen of the hydroxyl groups of ι-CGN and the hydrogen of the amine groups (B) of PAni acting as weak acids.

Finally, the peak at 1131 cm^{-1} was attributed to the vibration mode of the $-NH^{+}$ ion and to the asymmetric stretching vibration of SO_4^{-} ion showing the ionic interaction among aniliniun and sulfate ions (Trchová & Stejskal, 2011). This last band is very important as it confirms the ionic interaction between PAni and ι-CGN. In conclusion, based on the previous discussion on infrared spectroscopy, two types of interaction between ι-CGN and PAni can be established (Fig. 4). The first type, the electrostatic interaction between the sulfate groups of ι-CGN and the amino groups of PAni and the second, the hydrogen bonding between the hydroxyl group of ι-CGN and the imine hydrohalide (Q) of PAni. Consequently, both kinds of interactions are responsible for the formation of the interpenetrated polymer network, as observed in aqueous phase (hydrogel formation).

3.3. Thermal stability

Thermogravimetric analysis was performed to evaluate the stability of the composites and to determine how the interaction between PAni and ι-CGN could influence stability. TGA curves and the derivative of weight loss (DTG) curves are shown in Fig. 5 for all biocomposites and blanks of PAni and ι-CGN analyzed in argon atmosphere and heating rate of 10 °C min^{-1}. The derivative of weight loss (DTG) curves of all composites showed at least three significant thermal events (Fig. 5c and d). In the literature, several works dealing with the thermal stability of PAni (emeraldine salt) depending on the dopant used have been reported (Abell, Pomfret, Adams, & Monkman, 1997; Li & Wan, 1998). Besides some authors found a three-step decomposition process of PAni doped by acids (Ansari & Keivani, 2006; Lee & Char, 2002). They suggest that the initial stages of weight loss are due to the volatilization of water molecules and oligomers, as well as unreacted monomer elimination, subsequently, at higher temperatures the dopant acid is lost and finally at more extreme temperatures the polymer chain break can lead to production of gases such as acetylene and ammonia. The thermal behavior of blank PAni is similar to that reported in the literature, presenting an initial decomposition up to 150 °C, a second decomposition in a range of 150–300 °C and the last decomposition occurs at *ca.* 400 °C.

The profile of ι-CGN shows the first stage (60–150 °C) may be attributed to water evaporation, and chemisorbed water through hydrogen bonds with a 10.5% weight loss. The second stage (170–230 °C) is associated with sulfur dioxide leaving and carbohydrate backbone fragmentation (Freile-Pelegrín, Azamar, & Robledo, 2011; Vinceković et al., 2010). It also presents an abrupt thermal decomposition at 185 °C with weight loss of 21% and another one of 76.7% weight loss that is continuous almost without variation until

Table 2
Conductivity of PAni/ι-CGN biocomposites.

Sample	PAni [a] (wt%)	$T_{50\%}$ [b] (°C)	Conductivity (S cm^{-1})
PAni	–	342	4.62×10^{-1}
ι-CGN	–	313	1.36×10^{-8}
C1	21.2	247	1.59×10^{-3}
C2	28.7	314	6.97×10^{-3}
C3	37.0	324	5.16×10^{-2}
C4	50.5	358	5.98×10^{-2}
C5	62.6	408	6.41×10^{-2}
C6	81.3	411	8.51×10^{-2}

[a] PAni content in the biocomposites calculated using Eq. (1).
[b] The temperature at which the weight loss is 50% (see Supplementary Material Section, Fig. S3).

800 °C. κ-CGN shows similar behavior but with some small differences (Mishra, Tripathy, & Behari, 2008). The third stage is related to polysaccharide decomposition.

As observed, the biocomposites presented similar decomposition profiles to PAni and ι-CGN. The biocomposites presented multiple decomposition transitions in the range 200–600 °C (see Supplementary Material Section, Fig. S3). Analysis of the decomposition peak at 190 °C in the biocomposites shows that sulfate groups are doping PAni due to the change in peak shape in relation to sharp peak of the ι-CGN, which is broad, with initial decomposition temperature of approximately 150 °C and a maximum decomposition temperature between ι-CGN (185 °C) and PAni (198 °C), indicating that sulfate groups in the biocomposite C1 to C6 have a thermal decomposition mechanism different than the ι-CGN, by the ionic interaction with PAni. In addition, analysis at 50% weight loss indicated improvements in thermal stability with the increment of PAni loading in the biocomposite. Table 2 shows the decomposition temperatures of the biocomposites at 50% weight loss; as seen, it is clear that for higher content of PAni in the biocomposite the thermal stability improves.

3.4. Electrical properties

3.4.1. Electro-activity

Fig. 6 shows voltammograms of PAni/ι-CGN biocomposites recorded at a sweep rate of 50 mV s^{-1}, in 0.1 M H_2SO_4 aqueous solution. First, the biocomposites were hydrated in distilled warm water to be deposited on the working electrodes in the form of gel; subsequently, the electrodes were left to dry at 40 °C for 24 h. As seen, two pairs of redox peaks of PAni corresponding, respectively, to leucoemeraldine/emeraldine and emeraldine/pernigraniline redox transitions were observed. The first oxidation peak, at 200 mV, was attributed to the oxidation of the fully reduced PAni (leucoemeraldine) to the radical cations (emeraldine salt) without the exchange of protons between the PAni film and the solution, but accompanied by the exchange of anions (Orata & Buttry, 1987). Whereas the second oxidation peak, at 640 mV, was attributed to the oxidation of the radical cations (emeraldine salt) to pernigraniline, accompanied by the exchange of protons, and *vice versa* for their corresponding reduction peaks (Mu, 2010). In addition, the anodic peak, at 300 mV, represents the formation of benzoquinone (pernigraniline) (Li, Pang, Peng, Wang, Cui, & Zhang, 2005). The voltammetric behavior was similar to those reported in literature for other PAni biocomposites (Peng, Ma, Ying, Wang, Huang, & Lei, 2012). Oxidation–reduction transitions of biocomposites C1–C4 can be clearly observed in Supplementary Material in Figs. S4 and S5, respectively.

3.4.2. Electro-conductivity

The electro-conductivity of PAni/ι-CGN biocomposites and blanks of PAni and ι-CGN determined by the 4-probe technique

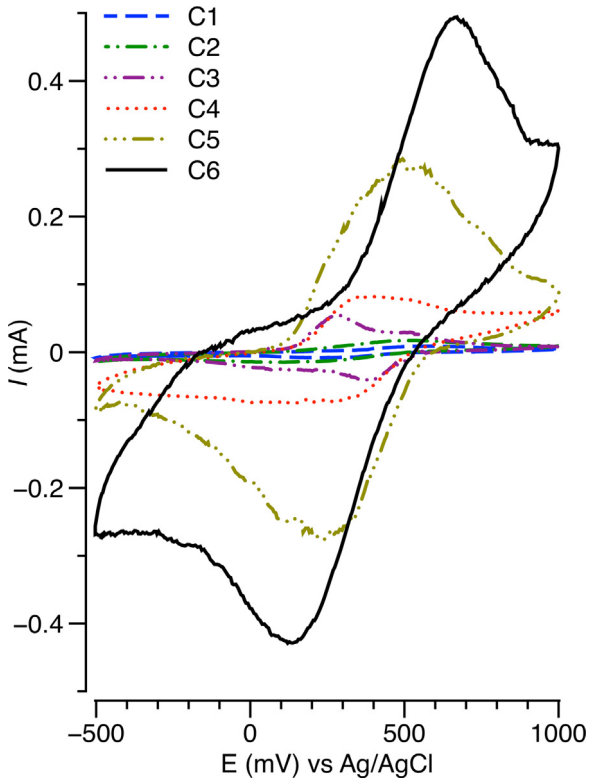

Fig. 6. Voltammograms of the PAni/ι-CGN biocomposites (C1 – 0.05 M, C2 – 0.1 M, C3 – 0.15 M, C4 – 0.2 M, C5 – 0.25 M, and C6 – 0.5 M).

is shown in Table 2. Before forming the pellets, the powder was dried at 40 °C for 48 h under reduced pressure in order to remove volatile substances. As observed, both the biocomposites and the pure PAni exhibited conductivity in the order of semiconductors, whereas ι-CGN is highly resistive. The biocomposites of PAni loading of 21.2 and 28.7 wt% exhibited conductivity in the order of 10^{-3} S cm^{-1}; while conductivity for the composites with the higher PAni contents was in the order of 10^{-2} S cm^{-1}. In the case of the polyaniline/κ-CGN biocomposites reported by Leppänen et al. (2013), the conductivity depended on the sulfate–aniline ratio; thus for the ratio of 1:2 the conductivity was 5×10^{-3} S cm^{-1}, whereas for the ratio of 1:1 the conductivity dropped to 6×10^{-7} S cm^{-1}. The amount of anionic groups present in the ι-CGN is approximately 32% (3.3 mmol g^{-1}) (Imeson, 2000). The ratio of anionic group to aniline used varied from 1:30 to 1:300 showing conductivities in the range of 1.59×10^{-3} to 8.51×10^{-2}. Concerning biocomposites of PAni with other polysaccharides we can mention, for example, that the conductivity of substituted PAni/chitosan (Ch) composites, reported by Uygun et al. (Yavuz, Uygun, & Bhethanabotla, 2009) were, respectively, of 7.73×10^{-5}, 1.68×10^{-4}, 6.84×10^{-6}, and 1.53×10^{-4} S cm^{-1} for PAni/Ch, poly(N-ethylaniline)/Ch, poly(N-methylaniline)/Ch, and poly(2-ethylaniline)/Ch composites. Additionally, in the paper by Youssef, El-Samahy, and Abdel Rehim (2012), the conductivity (S cm^{-1}) of PAni/rice straw fibers was 1.56×10^{-10} (2.5 wt% PAni), 4.56×10^{-7} (5 wt% PAni), 2.5×10^{-5} (10 wt% PAni), and for PAni/unbleached bagasse, 4.8×10^{-11} (2.5 wt% PAni), 1.8×10^{-7} (5 wt% PAni), 1.3×10^{-5} (10% PAni). As seen, the conductivity of these biocomposites is lower than those reported here, under the consideration that the loading of conducting polymer was higher. To conclude this section, we can mention that the biocomposites presented adequate properties for the development of practical applications based on electro-activity or electrical conductivity or both properties combined. Additionally, applications in the biomaterials field

are also possible thanks to the biological nature of the substrate (Grenha et al., 2010; Sjöberg, Persson, & Caram-Lelham, 1999).

4. Conclusions

Six polyaniline/ι-carrageenan biocomposites were synthesized by *in situ* methodology through an oxidative polymerization using ammonium persulfate as the oxidizing agent. The products exhibited the behavior of a cross-linked ionic hydrogel which suggested ionic interaction occurred between PAni and ι-carrageenan, and not only a simple physical interaction. Such physical behavior was supported by infrared spectroscopy as the band at 1131 cm^{-1} made clear the formation of anilinium sulfate ionic groups. Additionally, biocomposite electro-conductivity, determined by the 4-probe methodology, indicated values in the semiconductor range (10^{-3} to 10^{-2} $S\,cm^{-1}$), whereas electro-activity, in sulfuric acid as the electrolyte, exhibited in all cases the different oxidation–reduction transitions of PAni. Both electro-conductivity and electro-activity were dependent of PAni loading. Finally, it is worth saying considering that the electrical properties of these biomaterials can be affected; for instance, by changes in pH or humidity such that biosensor design, storage energy, and biomaterials are possible.

Acknowledgements

The authors thank Daniel Lardizabal, Carlos Ornelas and Luis de la Torre for their helpful collaboration during this research. We also thank Laboratorio Nacional de Nanotecnología for the assistance in microscopy analysis.

Appendix A. Supplementary data

Supplementary data associated with this article can be found, in the online version, at http://dx.doi.org/10.1016/j.carbpol.2014.03.068.

References

Abell, L., Pomfret, S. J., Adams, P. N., & Monkman, A. P. (1997). Thermal studies of doped polyaniline. *Synthetic Metals*, *84*(1–3), 127–128.

Al-Alawi, A. A., Al-Marhubi, I. M., Al-Belushi, M. S. M., & Soussi, B. (2011). Characterization of carrageenan extracted from Hypnea bryoides in Oman. *Marine Biotechnology*, *13*(5), 893–899.

Ansari, R., & Keivani, M. B. (2006). Polyaniline conducting electroactive polymers thermal and environmental stability studies. *E-Journal of Chemistry*, *3*(4), 202–217.

Bagheri, M., Didehban, K., Razmi, H., & Entezami, A. A. (2004). Determination of percolation threshold electroactivity and phase behavior study on conducting blends of thermotropic polyesters and polyaniline. *Polymers for Advanced Technologies*, *15*(12), 731–737.

Cai, L. T., & Chen, H. Y. (1998). Preparation and electro-activity of polyaniline/poly(acrylic acid) film electrodes modified by platinum microparticles. *Journal of Applied Electrochemistry*, *28*(2), 161–166.

Chao, L., Han, Y.-K., Hiseh, B.-Z., Huang, Y.-J., Hsieh, T.-H., Lin, C.-M., et al. (2008). Conducting polymer blends prepared from polyaniline with n-dodecylbenzenesulfonic acid zinc salt as the secondary dopant. *Journal of Applied Polymer Science*, *108*(6), 3516–3522.

Chopin, T., & Whalen, E. (1993). A new and rapid method for carrageenan identification by FT IR diffuse reflectance spectroscopy directly on dried, ground algal material. *Carbohydrate Research*, *246*(1), 51–59.

Coggins, C., Blanchard, K., Alvarez, F., Brache, V., Weisberg, E., Kilmarx, P. H., et al. (2000). Preliminary safety and acceptability of a carrageenan gel for possible use as a vaginal microbicide. *Sexually Transmitted Infections*, *76*(6), 480–483.

Di Rosa, M. (1972). Biological properties of carrageenan. *Journal of Pharmacy and Pharmacology*, *24*(2), 89–102.

Ebrahim, S. M., Kashyout, A. B., & Soliman, M. M. (2007). Electrical and structural properties of polyaniline/cellulose triacetate blend films. *Journal of Polymer Research*, *14*(5), 423–429.

Freile-Pelegrín, Y., Azamar, J. A., & Robledo, D. (2011). Preliminary characterization of carrageenan from the red seaweed Halymenia floresii. *Journal of Aquatic Food Product Technology*, *20*(1), 73–83.

Freile-Pelegrín, Y., & Robledo, D. (2008). Carrageenan of *Eucheuma isiforme* (Solieriaceae, Rhodophyta) from Nicaragua. *Journal of Applied Phycology*, *20*(5), 537–541.

Fujishima, M., Matsuo, Y., Takatori, H., & Uchida, K. (2008). Proton-conductive acid-base complex consisting of κ-carrageenan and 2-mercaptoimidazole. *Electrochemistry Communications*, *10*(10), 1482–1485.

Gaweł, K., Karewicz, A., Bielska, D., Szczubiałka, K., Rysak, K., Bonarek, P., et al. (2013). A thermosensitive carrageenan-based polymer: Synthesis, characterization and interactions with a cationic surfactant. *Carbohydrate Polymers*, *96*(1), 211–217.

Gómez-Ordóñez, E., & Rupérez, P. (2011). FTIR-ATR spectroscopy as a tool for polysaccharide identification in edible brown and red seaweeds. *Food Hydrocolloids*, *25*(6), 1514–1520.

Grenha, A., Gomes, M. E., Rodrigues, M., Santo, V. E., Mano, J. F., Neves, N. M., et al. (2010). Development of new chitosan/carrageenan nanoparticles for drug delivery applications. *Journal of Biomedical Materials Research Part A*, *92*(4), 1265–1272.

Haberko, J., Bernasik, A., Włodarczyk-Miśkiewicz, J., Łużny, W., Raczkowska, J., Rysz, J., et al. (2005). The structure of thin films of polyaniline/polystyrene polymer blends studied by SIMS. *Fibres & Textiles in Eastern Europe*, *13*(5), 103–106.

Hilliou, L., Larontonda, F. D. S., Sereno, A. M., & Gonçalves, M. P. (2006). Thermal and viscoelastic properties of kappa/iota-hybrid carrageenan gels obtained from the Portuguese seaweed Mastocarpus stellatus. *Journal of Agricultural and Food Chemistry*, *54*(20), 7870–7878.

Hu, W., Chen, S., Yang, Z., Liu, L., & Wang, H. (2011). Flexible electrically conductive nanocomposite membrane based on bacterial cellulose and polyaniline. *Journal of Physical Chemistry B*, *115*(26), 8453–8457.

Imeson, A. P. (2000). Carrageenan. In G. O. Phillips, & P. A. Williams (Eds.), *Handbook of hydrocolloids* (pp. 87–102). England: Woodhead Publishing Limited.

Lee, D., & Char, K. (2002). Thermal degradation behavior of polyaniline in polyaniline/Na^+-montmorillonite nanocomposites. *Polymer Degradation and Stability*, *75*(3), 555–560.

Lee, H.-J., Chung, T.-J., Kwon, H.-J., Kim, H.-J., & Tze, W. T. Y. (2012). Fabrication and evaluation of bacterial cellulose-polyaniline composites by interfacial polymerization. *Cellulose*, *19*(4), 1251–1258.

Leppänen, A.-S., Xu, C., Liu, J., Wang, X., Pesonen, M., & Willför, S. (2013). Anionic polysaccharides as templates for the synthesis of conducting polyaniline and as structural matrix for conducting biocomposites. *Macromolecualar Rapid Communications*, *34*(13), 1056–1061.

Li, G., Pang, S., Peng, H., Wang, Z., Cui, Z., & Zhang, Z. (2005). Templateless and surfactantless route to the synthesis of polyaniline nanofibers. *Journal of Polymer Science Part A: Polymer Chemistry*, *43*(17), 4012–4015.

Li, W., & Wan, M. (1998). Stability of polyaniline synthesized by a doping–dedoping–redoping method. *Journal of Applied Polymer Science*, *71*(4), 615–621.

Lim, Y.-M., Gwon, H.-J., Choi, J.-H., Shin, J., Nho, Y.-C., Jeong, S. I., et al. (2010). Preparation and biocompatibility study of gelatin/kappa-carrageenan scaffolds. *Macromolecular Research*, *18*(1), 29–34.

Liu, X., Zhou, W., Qian, X., Shen, J., & An, X. (2013). Polyaniline/cellulose fiber composite prepared using persulfate as oxidant for Cr(VI)-detoxification. *Carbohydrate Polymers*, *92*(1), 659–661.

Lü, Q., Wang, C., & Cheng, X. (2010). One-step preparation of conductive polyaniline-lignosulfonate composite hollow nanospheres. *Microchimica Acta*, *169*(3–4), 233–239.

Luo, J., Jiang, S., Wu, Y., Chen, M., & Liu, X. (2012). Synthesis of stable aqueous dispersion of graphene/polyaniline composite mediated by polystyrene sulfonic acid. *Journal of Polymer Science Part A: Polymer Chemistry*, *50*(23), 4888–4894.

Mirmohseni, A., Salari, D., & Nabavi, R. (2006). Preparation of conducting polyaniline/nylon 6. *Iranian Polymer Journal*, *15*(3), 259–264.

Mishra, D. K., Tripathy, J., & Behari, K. (2008). Synthesis of graft copolymer (k-carrageenan-g-N,N-dimethylacrylamide) and studies of metal ion uptake, swelling capacity and flocculation properties. *Carbohydrate Polymers*, *71*(4), 524–534.

Mu, S. (2010). Nanostructured polyaniline synthesized using interface polymerization and its redox activity in a wide pH range. *Synthetic Metals*, *160*(17–18), 1931–1937.

Müller, D., Mandelli, J. S., Marins, J. A., Soares, B. G., Porto, L. M., Rambo, C. R., et al. (2012). Electrically conducting nanocomposites: Preparation and properties of polyaniline (PAni)-coated bacterial cellulose nanofibers (BC). *Cellulose*, *19*(5), 1645–1654.

Orata, D., & Buttry, D. A. (1987). Determination of ion populations and solvent content as functions of redox state and pH in polyaniline. *Journal of the American Chemical Society*, *109*(12), 3574–3581.

Paul, R. K., & Pillai, C. K. S. (2000). Melt/solution processable conducting polyaniline with novel sulfonic acid dopants and its thermoplastic blends. *Synthetic Metals*, *114*(1), 27–35.

Peng, H., Ma, G., Ying, W., Wang, A., Huang, H., & Lei, Z. (2012). In situ synthesis of polyaniline/sodium carboxymethyl cellulose nanorods for high-performance redox supercapacitors. *Journal of Power Sources*, *211*(1), 40–45.

Pereira da Silva, J. E., Córdoba de Torresi, S. I., & Torresi, R. M. (2007). Polyaniline/poly(methylmethacrylate) blends for corrosion protection: The effect of passivating dopants on different metals. *Progress in Organic Coatings*, *58*(1), 33–39.

Pereira, L., & Mesquita, J. F. (2003). Carrageenophytes of occidental Portuguese coast: 1. Spectroscopic analysis in eight carrageenophytes from Buarcos Bay. *Biomolecular Engineering*, *20*(4–6), 217–222.

Pereira, L., Sousa, A., Coelho, H., Amado, A. M., & Ribeiro-Claro, P. J. A. (2003). Use of FTIR, FT-Raman and 13C-NMR spectroscopy for identification of some seaweed phycocolloids. *Biomolecular Engineering*, *20*(4–6), 223–228.

Pourjavadi, A., Harzandi, A. M., & Hosseinzadeh, H. (2004). Modified carrageenan. 3. Synthesis of a novel polysaccharide-based superabsorbent hydrogel via graft copolymerization of acrylic acid onto kappa-carrageenan in air. *European Polymer Journal*, *40*(7), 1363–1370.

Prasad, K., & Kadokawa, J. (2010). Preparation of composite materials composed of i-carrageenan and polymeric ionic liquids. *Polymer Composite*, *31*(5), 799–806.

Pud, A., Ogurtsov, N., Korzhenko, A., & Shapoval, G. (2003). Some aspects of preparation methods and properties of polyaniline blends and composites with organic polymers. *Progress in Polymer Science*, *28*(12), 1701–1753.

Qaiser, A. A., Hyland, M. M., & Patterson, D. A. (2011). Surface and charge transport characterization of polyaniline-cellulose acetate composite membranes. *Journal of Physical Chemistry B*, *115*(7), 1652–1661.

Rinaudo, M. (2008). Main properties and current applications of some polysaccharides as biomaterials. *Polymer International*, *430*(April 2007), 397–430.

Roy, S., Fortier, J. M., Nagarajan, R., Tripathy, S., Kumar, J., Samuelson, L. A., et al. (2002). Biomimetic synthesis of a water soluble conducting molecular complex of polyaniline and lignosulfonate. *Biomacromolecules*, *3*(5), 937–941.

Šeděnková, I., Trchová, M., Blinova, N. V., & Stejskal, J. (2006). In-situ polymerized polyaniline films. Preparation in solutions of hydrochloric, sulfuric, or phosphoric acid. *Thin Solid Films*, *515*(4), 1640–1646.

Šeděnková, I., Trchová, M., & Stejskal, J. (2008). Thermal degradation of polyaniline films prepared in solutions of strong and weak acids and in water-FTIR and Raman spectroscopic studies. *Polymer Degradation and Stability*, *93*(12), 2147–2157.

Sharma, A., Bhat, S., Vishnoi, T., Nayak, V., & Kumar, A. (2013). Three-dimensional supermacroporous carrageenan-gelatin cryogel matrix for tissue engineering applications. *BioMed Research International*, 1–15. Article ID 478279

Shi, Z., Zang, S., Jiang, F., Huang, L., Lu, D., Ma, Y., et al. (2012). In situ nanoassembly of bacterial cellulose-polyaniline composites. *RSC Advances*, *2*(3), 1040.

Šimkovic, I. (2013). Unexplored possibilities of all-polysaccharide composites. *Carbohydrate Polymers*, *95*(2), 697–715.

Sjöberg, H., Persson, S., & Caram-Lelham, N. (1999). How interactions between drugs and agarose-carrageenan hydrogels influence the simultaneous transport of drugs. *Journal of Controlled Release*, *59*(3), 391–400.

Socrates, G. (2001). *Infrared and Raman characteristic group frequencies* (3rd ed.). New York: John Wiley & Sons Ltd., pp. 94–98, 107–113, 122–123, 157–167, 176–177.

Sun, L., Shi, Y., Chu, L., Xu, X., & Liu, J. (2012). Preparation of polyaniline coated polystyrene-microparticles and the further fabrication of hollow polyaniline microspheres. *Journal of Applied Polymer Science*, *126*(3), 870–876.

Trchová, M., Šeděnková, I., Tobolková, E., & Stejskal, J. (2004). FTIR spectroscopic and conductivity study of the thermal degradation of polyaniline films. *Polymer Degradation and Stability*, *86*(1), 179–185.

Trchová, M., & Stejskal, J. (2011). Polyaniline: The infrared spectroscopy of conducting polymer nanotubes (IUPAC Technical Report). *Pure and Applied Chemistry*, *83*(10), 1803–1817.

Tsutsumi, H., Yamashita, S., & Oishi, T. (1997). Preparation of polyaniline-poly(p-styrenesulfonic acid) composite by post-polymerization and application as positive active material for a rechargeable lithium battery. *Journal of Applied Electrochemistry*, *27*(4), 477–481.

Turquois, T., Acquistapace, S., Vera, F. A., & Welti, D. H. (1997). Composition of carrageenan blends inferred from 13C-NMR and infrared spectroscopic analysis. *Carbohydrate Polymers*, *31*(1996), 269–278.

Tuvikene, R., Truus, K., Robal, M., Pehk, T., Kailas, T., Vaher, M., et al. (2009). Structure and thermal stability of pyruvated carrageenans from the red alga *Coccotylus truncatus*. *Carbohydrate Research*, *344*(6), 788–794.

Van, F. (2002). Carrageenan: A food-grade and biocompatible support for immobilisation techniques. *Advanced Synthesis Catalysis*, *344*(8), 815–835.

Vega-Rios, A., Hernández-Escobar, C. A., Zaragoza-Contreras, E. A., & Kobayashi, T. (2013). Electrical and electrochemical properties of polystyrene/polyaniline core–shell materials prepared with the use of a reactive surfactant as the polyaniline shell precursor. *Synthetic Metals*, *167*(March), 64–71.

Vinceković, M., Pustak, A., Tusek-Bozić, L., Liu, F., Ungar, G., Bujan, M., et al. (2010). Structural and thermal study of mesomorphic dodecylammonium carrageenates. *Journal of Colloid and Interface Science*, *341*(1), 117–123.

Volery, P., Besson, R., & Schaffer-Lequart, C. (2004). Characterization of commercial carrageenans by Fourier transform infrared spectroscopy using single-reflection attenuated total reflection. *Journal of Agricultural and Food Chemistry*, *52*(25), 7457–7463.

Wang, X., Liu, J., Feng, X., Guo, M., & Sun, D. (2008). Fabrication of hollow Fe3O4-polyaniline spheres with sulfonated polystyrene templates. *Materials Chemistry and Physics*, *112*(2), 319–321.

Yavuz, A. G., Uygun, A., & Bhethanabotla, V. R. (2009). Substituted polyaniline/chitosan composites: Synthesis and characterization. *Carbohydrate Polymers*, *75*(3), 448–453.

Yavuz, A. G., Uygun, A., & Kaplan Can, H. (2011). The effect of synthesis media on the properties of substituted polyaniline/chitosan composites. *Carbohydrate Research*, *346*(14), 2063–2069.

Youssef, A. M., El-Samahy, M. A., & Abdel Rehim, M. H. (2012). Preparation of conductive paper composites based on natural cellulosic fibers for packaging applications. *Carbohydrate Polymers*, *89*(4), 1027–1032.